

DEVELOPMENT OF TIME DELAY CURRENT CONTROL FOR LEAD ACID  
BATTERY 12 V DC BY USING ARDUINO

NURUL SYAZRAH BINTI MAT YATIM

The thesis is to submit in  
fulfillment of the requirement for the award of  
Degree of Master Electrical Engineering

Faculty of Electrical and Electronic Engineering  
Universiti Tun Hussein Onn Malaysia

JULY 2014

## ABSTRACT

Development of time delay current control for lead acid battery 12 V dc by using Arduino is the aim of this thesis. The development problem is necessary before applying control techniques to guarantee the execution of any task according to a desired input with minimum error. The main objective of this thesis is to design the time delay has on the performance of a current controlled for the buck-boost converter. The time delay controller is generally regarded as a nuisance to a control system. In addition, the performance of the Arduino and MATLAB as a signal processing device interface time is used. The feedback of open loop and closed loop time delay controller is also been analyzed. Based on results, the experiment of closed loop hardware gives better results than simulation in terms of output current. Through this study it is proved that the time delay controller is successfully designed to control current for lead acid battery.

## ABSTRAK

Pembangunan bagi masa tunda kawalan arus untuk asid plumbum bateri 12 V DC dengan menggunakan arduino adalah matlamat tesis ini. Masalah berkenaan dengan pembangunan diperlukan sebelum mengaplikasikan teknik kawalan untuk menjamin pelaksanaan apa-apa mengikut input yang dikehendaki dengan kesilapan yang minimum. Objektif utama projek ini adalah untuk mereka masa yang kelewatan mempunyai mengenai prestasi semasa dikawal. Pengawal kelewatan masa biasanya dianggap sebagai gangguan kepada sistem kawalan. Tambahan lagi, prestasi arduino dan MATLAB sebagai peranti isyarat kawalan pemprosesan masa ingin ditingkatkan. Maklumbalas gelung terbuka dan gelung tertutup kawalan masa tunda juga telah dianalisis. Berdasarkan keputusan yang diperolehi, eksperimen terhadap perkakasan gegelung tertutup memberikan keputusan yang lebih baik daripada simulasi dari segi keluaran arus. Melalui kajian ini dibuktikan bahawa kawalan masa tunda berjaya direka untuk mengawal arus bagi sistem pengecasan bateri.

## CONTENTS

|   |              |
|---|--------------|
| <b>TITLE</b>                                      | <b>I</b>     |
| <b>DECLARATION</b>                                | <b>II</b>    |
| <b>DEDICATION</b>                                 | <b>III</b>   |
| <b>ACKNOWLEDGEMENT</b>                            | <b>IV</b>    |
| <b>ABSTRACT</b>                                   | <b>V</b>     |
| <b>ABSTRAK</b>                                    | <b>VI</b>    |
| <b>CONTENTS</b>                                   | <b>VII</b>   |
| <b>LIST OF FIGURES</b>                            | <b>IX</b>    |
| <b>LIST OF TABLES</b>                             | <b>XII</b>   |
| <b>LIST OF SYMBOLS AND ABBREVIATIONS</b>          | <b>XIII</b>  |
| <br><b>CHAPTER 1</b>                              | <br><b>1</b> |
| <b>INTRODUCTION</b>                               | <b>1</b>     |
| 1.1 Project Background                            | 1            |
| 1.2 Problem Statement                             | 3            |
| 1.3 Objectives                                    | 3            |
| 1.4 Research Scope                                | 4            |
| <br><b>CHAPTER 2</b>                              | <br><b>5</b> |
| <b>LITERATURE REVIEW</b>                          | <b>5</b>     |
| 2.1 A Brief Review of Battery                     | 5            |
| 2.2 Single – Phase Buck – Boost Converter         | 8            |
| 2.3 Control Method between Buck-Boost and Battery | 10           |
| 2.4 Time Delay Control                            | 19           |
| 2.5 Arduino                                       | 21           |

|   |           |
|---|-----------|
| <b>CHAPTER 3</b>                              | <b>23</b> |
| <b>RESEARCH METHODOLOGY</b>                   | <b>23</b> |
| 3.1 Block Diagram of the Project              | 23        |
| 3.2 Flowchart of System                       | 24        |
| 3.3 Project Development                       | 26        |
| <b>CHAPTER 4</b>                              | <b>38</b> |
| <b>RESULT AND DISCUSSION</b>                  | <b>38</b> |
| 4.1 Open Loop Simulation Diagram and Result   | 38        |
| 4.2 Closed Loop Simulation Diagram and Result | 44        |
| 4.3 Open Loop Hardware and Result             | 49        |
| 4.4 Closed Loop Hardware and Result           | 59        |
| <b>CHAPTER 5</b>                              | <b>65</b> |
| <b>CONCLUSION AND RECOMMENDATION</b>          | <b>65</b> |
| 5.1 Conclusion                                | 65        |
| 5.2 Recommendations                           | 66        |
| REFERENCES                                    | 67        |
| <b>VITA</b>                                   | <b>70</b> |
| <b>APPENDIX A</b>                             | <b>71</b> |
| <b>APPENDIX B</b>                             | <b>73</b> |
| <b>APPENDIX C</b>                             | <b>74</b> |

## LIST OF FIGURES

|  |    |
|--|----|
| Figure 1.1: Block diagram of battery charger system                                | 2  |
| Figure 2.1: Load curve for Kyushu region in Japan August,2011                      | 8  |
| Figure 2.2: System block diagram   | 9  |
| Figure 2.3: Photovoltaic power system  | 10 |
| Figure 2.4: The Conventional dynamic model of buck - boost converter.              | 10 |
| Figure 2.5: Scheme of voltage-mode controlled boost DC/DC converter                | 11 |
| Figure 2.6: Time-delay introduced by PWM in voltage-mode control                   | 12 |
| Figure 2.7: Scheme of current-mode controlled boost DC/DC converter                | 12 |
| Figure 2.8: Illustration of the stability of current loop is stable when $D < 0.5$ | 13 |
| Figure 2.9: Common Buck – Boost circuit  | 13 |
| Figure 2.10: Common Buck circuit   | 14 |
| Figure 2.11: Common Boost circuit  | 14 |
| Figure 2.12 : Inductor current versus time   | 15 |
| Figure 2.13: Ridley’s model of the time-delay controller.                          | 19 |
| Figure 2.14: The Arduino board   | 22 |
| Figure 3.1: Block diagram of time delay control current for battery.               | 23 |
| Figure 3.2: Flowchart of the lead acid battery charger                             | 24 |
| Figure 3.3: The time delay control closed loop                                     | 25 |
| Figure 3.4: Buck – Boost converter circuit layout                                  | 26 |
| Figure 3.5: Hardware of Buck-Boost converter circuit.                              | 27 |
| Figure 3.6: Boost circuit diagram in buck – boost circuit                          | 28 |
| Figure 3.7 : Buck condition in Buck – boost circuit                                | 29 |
| Figure 3.8: Gate driver layout   | 32 |
| Figure 3.9: Hardware of Gate driver circuit  | 33 |
| Figure 3.10: Current sensor 50A layout   | 34 |
| Figure 3.11: Current sensor 50A  | 34 |

|   |    |
|---|----|
| Figure 3.12: Voltage sensor circuit                                       | 36 |
| Figure 3.13: Experiment set up  | 37 |
| Figure 4.1: Boost circuit diagram in buck – boost circuit                 | 39 |
| Figure 4.2: Open loop simulation diagram                                  | 39 |
| Figure 4.3: AND and OR gates block diagram                                | 40 |
| Figure 4.4: The simulink model of arduino for open loop diagram           | 41 |
| Figure 4.5: Output waveform of the gate driver when boost operation       | 41 |
| Figure 4.6: Output waveform of the gate driver when buck operation        | 42 |
| Figure 4.7: The output current for open loop simulation waveform          | 43 |
| Figure 4.8: Closed loop simulation diagram                                | 44 |
| Figure 4.9: The Simulink model for closed loop                            | 45 |
| Figure 4.10: The simulink model for the Analog to Digital converter (ADC) | 45 |
| Figure 4.11: The simulink model for current sensor by time delay control  | 46 |
| Figure 4.12: The output current for closed loop simulation waveform       | 47 |
| Figure 4.13: Pin 11 – constant input waveform when boost condition        | 49 |
| Figure 4.14: Pin 9 – PWM input waveform when boost condition              | 50 |
| Figure 4.15: Pin 11 – zero input waveform when buck condition             | 50 |
| Figure 4.16: Pin 9 – PWM input waveform when buck condition               | 51 |
| Figure 4.17: A switch SW1 output when boost condition                     | 51 |
| Figure 4.18: A switch SW2 output when boost condition                     | 52 |
| Figure 4.19: A switch SW1 output when buck condition                      | 52 |
| Figure 4.20: A switch SW2 output when buck condition                      | 53 |
| Figure 4.21: Graph $V_{out}$ when $V_{in}=10V$                            | 53 |
| Figure 4.22: Graph $V_{out}$ when $V_{in}=11V$                            | 53 |
| Figure 4.23: Graph $V_{out}$ when $V_{in}=12V$                            | 54 |
| Figure 4.24: Graph $V_{out}$ when $V_{in}=13V$                            | 54 |
| Figure 4.25: Graph $V_{out}$ when $V_{in}=14V$                            | 54 |
| Figure 4.26: Graph $V_{out}$ when $V_{in}=15V$                            | 54 |
| Figure 4.27: Graph $V_{out}$ when $V_{in}=16V$                            | 55 |
| Figure 4.28: Graph $V_{out}$ when $V_{in}=17V$                            | 55 |
| Figure 4.29: Graph $V_{out}$ when $V_{in}=18V$                            | 55 |

|  |    |
|--|----|
| Figure 4.30: The open loop hardware waveform                     | 56 |
| Figure 4.31: Graph IV characteristic for open loop hardware      | 58 |
| Figure 4.32: Closed Loop Hardware set up                         | 59 |
| Figure 4.33: Graph $V_{out}$ when $V_{in}=10V$                   | 60 |
| Figure 4.34: Graph $V_{out}$ when $V_{in}=11V$                   | 60 |
| Figure 4.35: Graph $V_{out}$ when $V_{in}=12V$                   | 60 |
| Figure 4.36: Graph $V_{out}$ when $V_{in}=13V$                   | 60 |
| Figure 4.37: Graph $V_{out}$ when $V_{in}=14V$                   | 61 |
| Figure 4.38: Graph $V_{out}$ when $V_{in}=15V$                   | 61 |
| Figure 4.39: Graph $V_{out}$ when $V_{in}=16V$                   | 61 |
| Figure 4.40: Graph $V_{out}$ when $V_{in}=17V$                   | 61 |
| Figure 4.41: Graph $V_{out}$ when $V_{in}=18V$                   | 62 |
| Figure 4.42: The closed loop hardware waveform                   | 62 |
| Figure 4.43: Graph IV characteristic of the closed loop hardware | 64 |



**LIST OF TABLES**

|  |    |
|--|----|
| Table 2.1: The comparison between rechargeable batteries | 6  |
| Table 2.2: The pros and cons of each charging method     | 18 |
| Table 3.1: List of component for buck-boost circuit      | 27 |
| Table 3.2: Switch condition for boost operation          | 28 |
| Table 3.3: Parameter characteristic for Boost circuit    | 29 |
| Table 3.4: Switch condition for buck operation           | 30 |
| Table 3.5: Parameter characteristic for Buck circuit     | 31 |
| Table 3.6: Lists of components for gate driver circuit   | 33 |
| Table 4.1: Truth table of OR gate                        | 40 |
| Table 4.2: Truth table of AND gate                       | 40 |
| Table 4.3: Open loop simulation result                   | 43 |
| Table 4.4: Closed loop simulation result                 | 47 |
| Table 4.5: The simulation result                         | 48 |
| Table 4.6: Open loop simulation and hardware result      | 57 |
| Table 4.7: Closed loop simulation and hardware result    | 63 |

## LIST OF SYMBOLS AND ABBREVIATIONS

|             |   |  |
|-------------|---|--|
| $r, r(t)$   | - | Reference input  |
| $e, e(t)$   | - | Error between the input signal and the output                        |
| $u, u(t)$   | - | Input applied by the controller to plant                             |
| $y, y(t)$   | - | Output of the closed loop control system                             |
| $G_p(s)$    | - | Plant transfer function  |
| $G_c(s)$    | - | Controller transfer function   |
| $G_d(s)$    | - | Disturbance input to output transfer function                        |
| $H(s)$      | - | Feedback measurement   |
| $D_t(s)$    | - | Disturbance input  |
| $v_a(t)$    | - | Input source voltage, [Volt]   |
| $i_a(t)$    | - | Armature current, [Ampere]   |
| $R_a$       | - | Armature resistance, [Ohm]   |
| $L_a$       | - | Electric inductance, [H]   |
| $T_i^{i-1}$ | - | Homogeneous transformation matrix of $I$ relative to $i-1$           |
| $K_P$       | - | Proportional gain  |
| $K_D$       | - | Derivative gain  |
| $K_I$       | - | Integral gain  |
| $T_I$       | - | Integral time constant   |
| $T_D$       | - | derivative time constant   |
| $t_r$       | - | Rising time, [sec]   |
| $t_s$       | - | Settling time, [sec]   |
| $\mu(u)$    | - | Membership function  |
| $\Phi$      | - | Null fuzzy set (Phi)   |
| $\Delta e$  | - | Change of the error  |
| $k_e$       | - | Scaling factor for error   |
| $k_{de}$    | - | Scaling factor for change of error                                   |
| $k_u$       | - | Scaling factor for output  |
| $n$         | - | Degree of freedom of robot manipulator ( $n$ -DOF robot manipulator) |

|            |   |                             |
|------------|---|-----------------------------|
| <i>i</i>   | - | Number of links             |
| <i>R</i>   | - | Number of the fuzzy rules   |
| <i>V</i>   | - | Voltage                     |
| <i>DC</i>  | - | direct current              |
| <i>PWM</i> | - | Pulse Width Modulation      |
| <i>ADC</i> | - | Analog to Digital Converter |
| <i>CC</i>  | - | Constant Current            |
| <i>CV</i>  | - | Constant Voltage            |
| <i>SOC</i> | - | State of Charge             |

## CHAPTER 1

### INTRODUCTION

#### 1.1 Project Background

There is a wide variety of batteries on the market today, which are Nickel Cadmium (NiCa/NiCd), Nickel Metal Hydride (NiMH), Lead acid and Lithium Ion (Li-Ion) batteries. The lead-acid battery is widely used as a supply of power because the maintenance is easy and it's convenient to be used [1]. However, as the repeated charging and discharging the capacity of lead-acid battery gets decreased, meanwhile, its life span become short as well. It's known that the charging process is the most important factor to the working life of lead-acid battery.

Power conversion system is constructed to improve performance or reliability, or attain a high system rating [2]. Energy can flow from the highest cell to the lowest cell with the isolated buck - boost DC – DC converter. The control scheme implements the balancing with the least quantity of switches and cost [3]. Buck - boost converters are frequently used as a battery charging/discharging circuit in many photovoltaic power system, automotive power system and spacecraft power system [4].

The control parameters for the digital compensation are designed and fine – tuned using the Arduino in MATLAB software. Theoretical predictions are confirmed with both MATLAB simulation and measurement on an experimental prototype converter. Because battery-charge control is a slow process, microcontrollers with embedded ADCs such as the Arduino can be used inexpensive, signal conditioning, and PWM modules to directly control the charger's power-conversion circuits.

Figure 1.1 shows the block diagram of battery charger system which consists of a power source, the buck – boost DC converter, control system and battery. Power source will supply an input DC voltage. Then, the voltage will be converted to the stable voltage by using buck –boost DC converter. The control system will be monitoring the data of input voltage and output current. A battery as a load in the battery charging system.

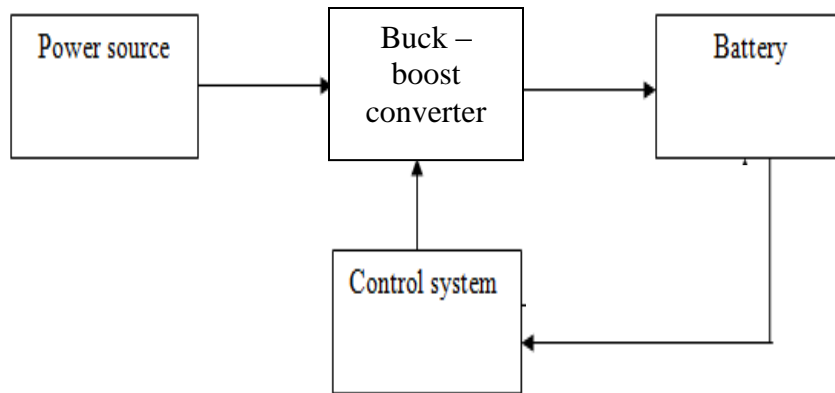


Figure 1.1: Block diagram of battery charger system

## 1.2 Problem Statement

To charge batteries, many battery charge strategies have been proposed. The constant-current constant - voltage charge strategy is the most popularly used one these days. However, a battery charge system with a high quality is still desired [5]. The controller such as PID, p-resonant, repetitive and time delay, fuzzy logic control and etc was applied in battery charge systems. Conventional controller has issued in handling charge current to increase battery charging performance.

In electrical vehicle applications power supply systems, the battery charger circuits require an output voltage which is usually less than the input voltage [2]. Regarding the battery condition, the buck – boost converter will work as a current source or as a voltage source. For the controller design the worst case to control switching of buck – boost converter has been taking into consideration. The output from buck – boost converter must be constant compare to an input which is variable.

## 1.3 Objectives

1. To design the time delay controller of a current controlled
2. To analyze the feedback of open and closed loop using time delay controller.
3. To enhance the performance of the Arduino and MATLAB for signal processing device interface time.
4. To design the gate driver circuit to control switching for a buck – boost converter.

## 1.4 Research Scope

1. The size of the battery is 12 V 7 Ah lead acid.
2. The size of bidirectional converter is 10 - 18 V input voltage, 12 V output voltages with filter inductor value is 10mH, Filter capacitor value is 47 $\mu$ F.
3. Perform simulation of time delay controller. This simulation will be carried out on MATLAB platform with Simulink as it user interface.
4. Analyze the performance of time delay controller.
5. Development and implements the hardware of current control of battery for time delay control using the Arduino

## CHAPTER 2

### LITERATURE REVIEW

#### 2.1 A Brief Review of Battery

Methods of fast charging of lead acid batteries have been studied and developed for the last 30 years. In 1973, there has been a publication outlining that fast charging has some chemical and physical effects on battery plates, and therefore reduces the battery life. These effects can be seen as gassing and heat generation [6]. It is desirable to be able to rapidly recharge its batteries within one hour or less. As is the case under any charging conditions, it is important to control the charge in order to maintain the batteries in good condition. The rise of temperature, the overcharge and gassing are more prone to occur during high-rate charging, charge control under these conditions is critical.

In recent years, the issues about greenhouse effect generated by carbon dioxide have been worried, so people know the importance of environmental protection. Common rechargeable batteries are NiMH battery, NiCd battery, lead-acid battery and Li-ion battery on the market that are shown in Table 2.1. Lead-acid battery is used in motor vehicles, industrial equipment and power-storage systems. NiMH battery and NiCd battery are used in cordless power tool and hybrid vehicles. Li-ion Battery is used in power packs portable electronics series. Because lead and cadmium are harmful for the environment and the human beings, lead-acid battery and NiCd batteries have been gradually replaced by NiMH battery. The NiMH battery with the conversion efficiency and problems with memory effect, have been replaced gradually by Li-ion battery. In



these batteries, lead- acid battery has a long history and is safe, reliable and affordable[7].

Table 2.1: The comparison between rechargeable batteries

| Type                      | Lead-acid battery | NiCad battery | NiMH battery | LiCoO <sub>2</sub> battery |
|---------------------------|-------------------|---------------|--------------|----------------------------|
| Nominal Operating Voltage | 2V                | 1.2V          | 1.2V         | 3.7V                       |
| Patent protection         | No                | No            | No           | No                         |
| Price                     | 1                 | 2             | 2.4          | 4                          |
| Security                  | Good              | Good          | Good         | Bad                        |
| Green product             | No                | No            | Yes          | Yes                        |
| Memory effect             | No                | Yes           | Yes          | Yes                        |
| Energy efficiency         | 60%               | 75%           | 70%          | 90%                        |
| Cycle life                | 400               | 500           | 500          | .500                       |
| Charge time               | 8hours            | 1.5Hours      | 4Hours       | 2-4Hours                   |
| Self-discharge            | 20%Month          | 30%Month      | 35%Month     | 10%Month                   |

The battery plays very important role and the energy converters are operated based upon battery online conditions like state of charge (SOC), terminal voltage, and temperature etc of the battery. Most of time, the lead-acid battery is used for this purpose. The modeling of the battery is a complex process because many phenomenon are occurred inside the battery during its life cycle for example self-discharging, gassing effect, diffusion process, acid stratification etc [8].

The charge ends when the battery capacity is reached and the battery is going to discharge to register more information about the efficiency of the complete process. The value of capacity for each battery is taken of a database where the battery life is stored. The combined charge strategies is used to obtain a high charge efficiency with considerable reduction of the charge time, as well as keep the battery temperature between reasonable values (maximum value 50°C) or not exceed the bubbling voltage (7.95 V, in these batteries). If the central cell temperature reaches 50°C the software pauses the process until the temperature goes down a program value, then the charge is resumed [9].

The cycle-life of lead-acid batteries can indeed be improved by the use of high charge currents. We are working in the development of electronic systems of fast charge lead-acid batteries and so that this system can optimize the yield and the useful life of the battery, it is needed to provide to the battery the necessary load and with the most appropriate strategy [10].

A typical demand curve is shown in Figure 2.1. Battery charging activities during daytime need to be somehow restricted, and most of the plug-in electric vehicle loads need to be allocated to nighttime. An ideal is to prevent any new peak load from exceeding the natural peak. To fill the overnight demand valley of the electrical grid off – line algorithms have been studied recently for single cycle [11].

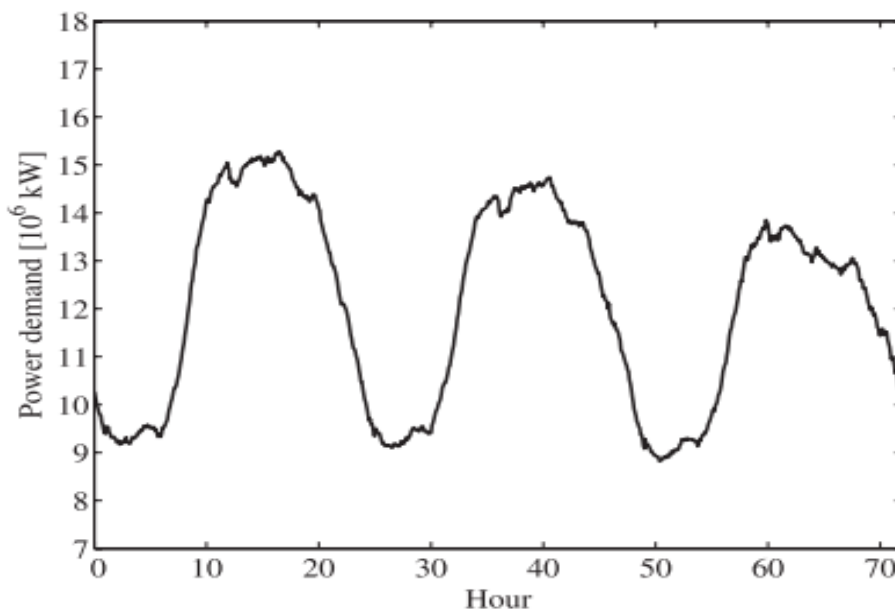


Figure 2.1: Load curve for Kyushu region in Japan August,2011

## 2.2 Single – Phase Buck – Boost Converter

Buck - boost converters are frequently used as a battery charging/discharging circuit in many photovoltaic power systems, automotive power systems, and spacecraft power system. In these applications, bidirectional converters often employ a multi-module structure in order to reduce the ripple component in the battery charging/discharging current. In particular the magnitude of the ripple component can be drastically shrunk by operating power modules with appropriate phase delays in their switch driving signals. This multi-module multi-phase operation reduces the switch current stress and inductor size. In addition, it could substantially improve the battery lifetime and system reliability [4].

Buck - Boost DC–DC converters allow the transfer of power between two DC sources in either direction. They are increasingly used in applications such as DC uninterruptible power supplies, battery chargers, multiplexed-battery systems, computer systems, aerospace systems, DC motor drives circuits and electric vehicles [12].

Buck converter and boost converter are usually used in maximum power point system because of their simplicity in structure and control scheme. Buck converter can generate a voltage below the input voltage, while boost converter steps up the input voltage to a higher voltage. While they are mostly used in high power PV system, both of them are not suitable for the application of energy-harvesting battery charger. Inverting buck-boost converters and Cuk converters are capable of converting supply voltages to both higher and lower voltages, but the polarity of the output voltage is opposite to the supply voltage, which makes it not applicable for multiple power source system [13].

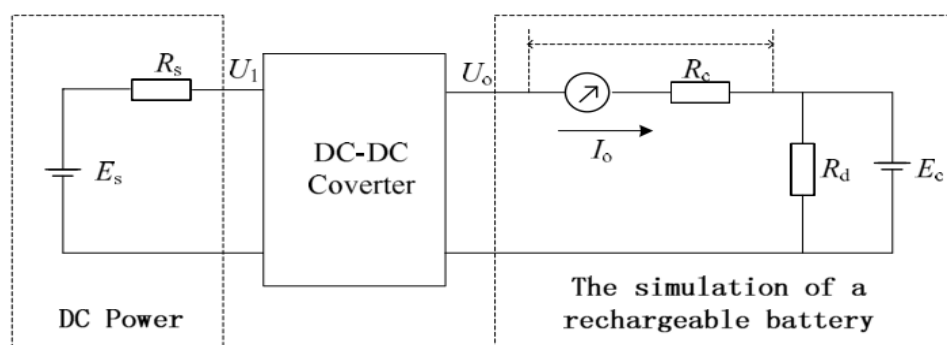


Figure 2.2: System block diagram

Therefore, a buck - boost DC-DC converter is one of the most important topics for power electronics. Figure 2.3 shows an example of its application. In these power system used in combination with buck – boost DC – DC converter and battery, the direction of the charge and discharge current is changed from time to time to perform power conversion between the different voltages. The batteries are connected to the buses with buck - boost DC-DC converters for ensuring a stable energy supply [14].

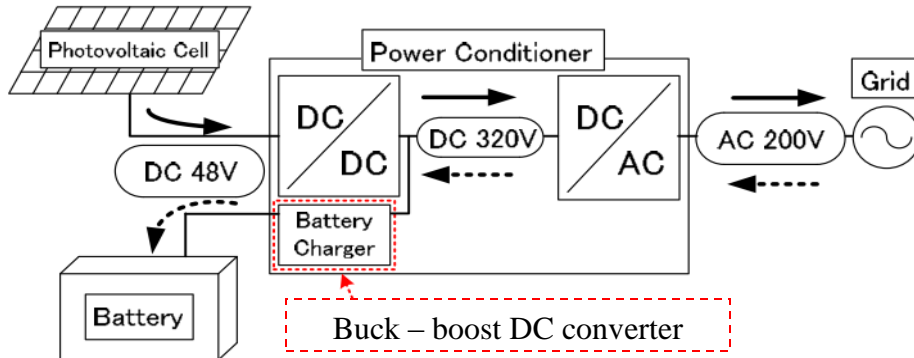


Figure 2.3: Photovoltaic power system

### 2.3 Control Method between Buck-Boost and Battery

A buck - boost DC – DC converter connects two sources/loads, it has two modes of operation (see Figure2.4): 1- Discharging mode; the power is fed forward from the battery to load. 2-Charging mode; where the power is fed back to the battery.

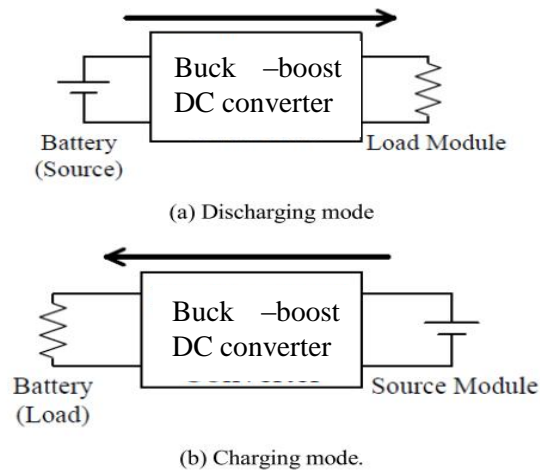


Figure 2.4: The Conventional dynamic model of buck - boost converter.

Using different takes charging methods influences the life of battery. It spends too much time and cost to charge batteries by the methods which are safe and high efficient according to the service manual that the battery manufacturer offered. Therefore, the characteristics of fast and less influence of the charging methods are proposed successively.

As shown in Figure 2.5, there is only the voltage feedback in voltage-mode control. Duty ratio  $d$  is determined by the comparison of the sawtooth waveform and the control voltage  $v_c$ , which is the amplified error of voltage reference  $v_r$  and the feedback voltage  $v_f$ . PWM transfers  $v_c$  to  $d$  [15].

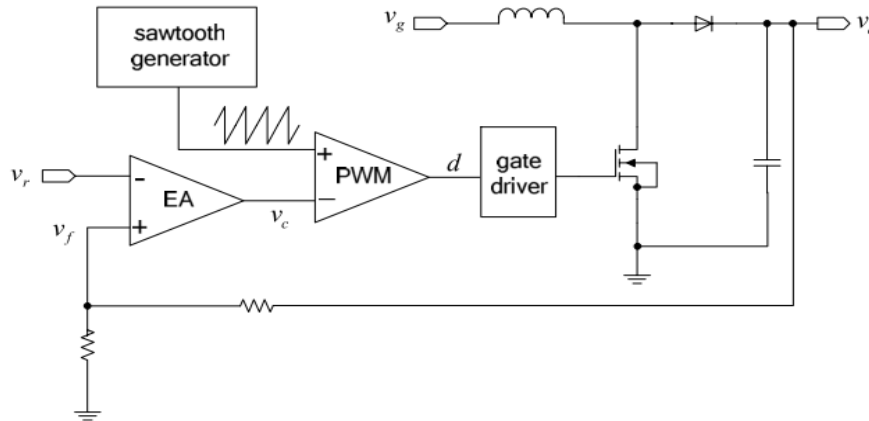


Figure 2.5: Scheme of voltage-mode controlled boost DC/DC converter

Figure 2.6 illustrates the time-delay  $\tau$  between  $v_c$  perturbation and the system response in the form of adjusting  $d$ . Thus, PWM in voltage-mode control is modeled as

$$F_m(s) = \frac{\hat{d}(s)}{\hat{v}_c(s)} = \frac{1}{S_e T_s} e^{-\tau s} \dots\dots\dots(2.1)$$

Where  $S_e$  is the slope of the sawtooth waveform,  $T_s$  is the switching period.

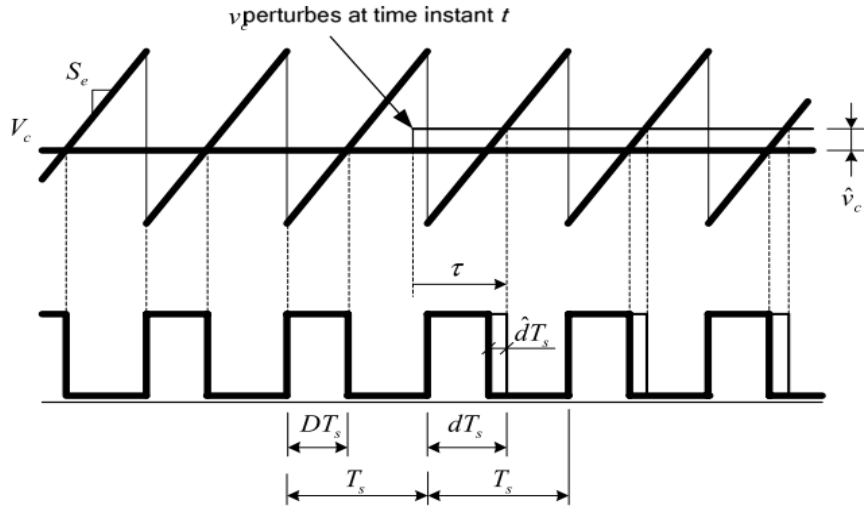


Figure 2.6: Time-delay introduced by PWM in voltage-mode control

The time-delay model of PWM in voltage-mode control

$$F_m(s) = \frac{1}{s_e T_s} e^{-\tau s} \Big|_{\tau \sim U[0, T]} \dots\dots(2.2)$$

Figure 2.7 shows that in current-mode control there is an additional current loop inside the outer voltage loop. The duty-ratio is no longer an independent variable but is controlled by the inductor – current  $i_L$ .

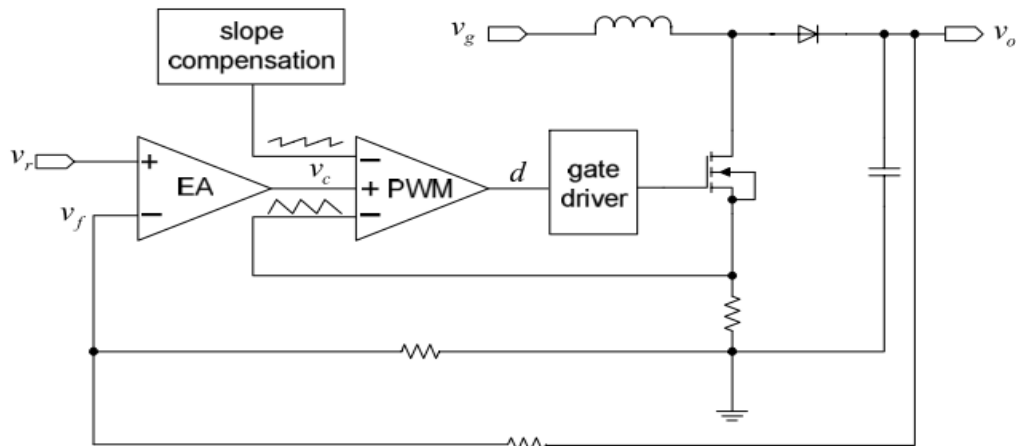


Figure 2.7: Scheme of current-mode controlled boost DC/DC converter

Assume each variable only perturbs in the small-signal limit, Figure 2.8 illustrates that the duty-ratio plays a decisive role in the stability of current loop, which is one of the most important issues of current-mode control. Similar as (2.1), the time-delay model of PWM operating in current-mode control is

$$F_m(s) = \frac{\hat{d}(s)}{\hat{v}_c(s)} = \frac{1}{(S_e + S_n)T_s} e^{-\tau s} \Big|_{\tau \sim U[0, T]} \dots\dots\dots(2.3)$$

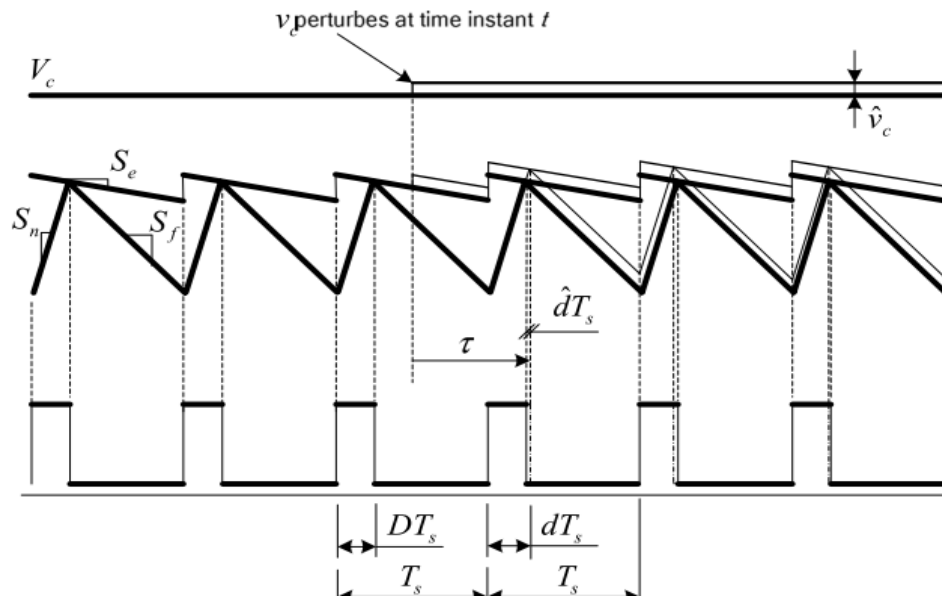


Figure 2.8: Illustration of the stability of current loop is stable when  $D < 0.5$

Figure 2.9 shows the common buck – boost circuit diagram. This circuit consist two switches, an inductor, two diodes, a capacitor and two resistors. If the input voltage is higher than reference voltage, the circuit will in buck condition as shown in Figure 2.10 while the input voltage is low than reference voltage, the circuit will be in boost condition as shown in Figure 2.11.

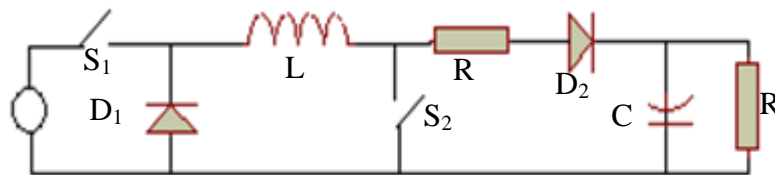


Figure 2.9: Common Buck – Boost circuit



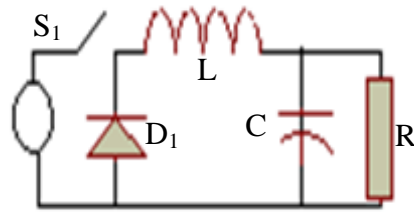


Figure 2.10: Common Buck circuit

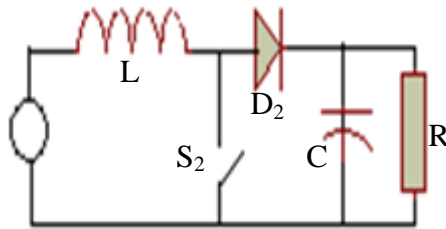


Figure 2.11: Common Boost circuit

For the boost condition, by using Kirchoff's Voltage Law, the voltage across the inductor,  $V_L$  is given by the difference between voltage supply,  $V_s$  and output voltage,  $V_o$ .

$$V_L = V_s - V_o \dots\dots\dots (2.4)$$

The inductor voltage,  $V_L$  is related to the change in current flowing through it according to the relation.

$$V_L = L \frac{di_L}{dt} \dots\dots\dots (2.5)$$

Equating  $V_L$  in both equation,

$$V_L = V_s - V_o = L \frac{di_L}{dt} \dots\dots\dots (2.6)$$

$$\frac{di_L}{dt} = \frac{V_s - V_o}{L} \dots\dots\dots (2.7)$$

Since  $\frac{di_L}{dt}$  is constant, the equation can rewrite as below:

$$\frac{di_L}{dt} = \frac{\Delta i_L}{\Delta t_1} = \frac{V_s - V_o}{L} \dots\dots\dots (2.8)$$

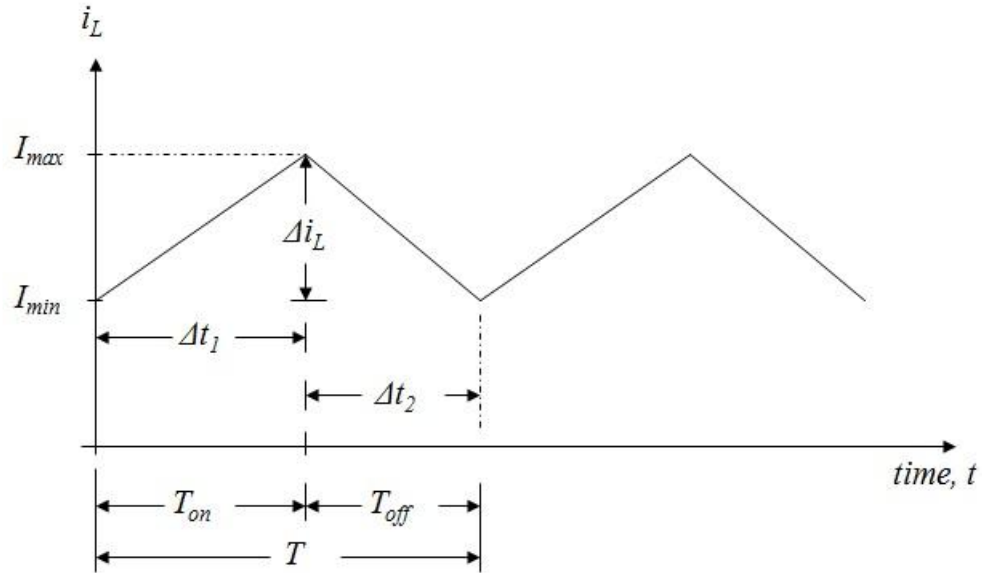


Figure 2.12 : Inductor current versus time

The duty cycle, D of the switch is defined as follows:

$$D = \frac{T_{on}}{T_{on} + T_{off}} = \frac{T_{on}}{T} \dots\dots\dots (2.9)$$

Equation can be rewritten as below:

$$\frac{\Delta i_L}{DT} = \frac{V_s - V_o}{L}$$

$$\Delta i_L = \left( \frac{V_s - V_o}{L} \right) DT \dots\dots\dots(2.10)$$

For an inductor value,

$$L_{min} = \frac{D(1-D)^2 R_L}{2f} \quad \dots \text{ where given } f = 10\text{kHz} \dots(2.11)$$

For a capacitor value,

$$C = \frac{D}{Rf \left( \frac{\Delta V_o}{V_{DC}} \right)} \dots\dots\dots(2.12)$$

For the buck condition, by using Kirchhoff's Voltage Law, the voltage across the inductor,  $V_L$  is given by the difference between voltage supply,  $V_s$  and output voltage,  $V_o$ .

$$V_L = -V_o \dots\dots\dots(2.13)$$

The inductor voltage,  $V_L$  is related to the change in current flowing through it according to the relation.

$$V_L = L \frac{di_L}{dt} \dots\dots\dots(2.14)$$

Equating  $V_L$  in both equation,

$$V_L = -V_o = L \frac{di_L}{dt}$$

$$\frac{di_L}{dt} = \frac{-V_o}{L} \dots\dots\dots(2.15)$$

Since  $\frac{di_L}{dt}$  is constant, the equation can rewrite as below:

$$\frac{di_L}{dt} = \frac{\Delta i_L}{\Delta t_2} = \frac{-V_o}{L} \dots\dots\dots(2.16)$$

By referring Figure 2.5,

$$\Delta t_2 \equiv T_{off} = (1 - D)T$$

$$\frac{\Delta i_L}{(1 - D)T} = \frac{-V_o}{L}$$

$$\Delta i_L = \frac{-V_o}{L}(1-D)T \dots\dots\dots(2.17)$$

The nett change in inductor current over the period T is zero, this condition requires that

$$|\Delta i_L|_{closed} = |\Delta i_L|_{opened}$$

Hence,

$$\left( \frac{V_s - V_o}{L} \right) = \frac{V_o}{L}(1-D)T \dots\dots\dots(2.18)$$

Solving for  $V_o$ :

$$V_o = DV_s \dots\dots\dots(2.19)$$

For an inductor value,

$$L_{min} = \frac{(1-D) R_L}{2f} \dots \text{ where given } f = 10\text{kHz} \quad (2.20)$$

For a capacitor value,

$$C = \frac{1-D}{8L \left( \frac{\Delta V_o}{V_{DC}} \right) f^2} \dots\dots\dots(2.21)$$

Table 2.2: The pros and cons of each charging method

| Method                                   | Advantage   | Disadvantage                                |
|--|---|---|
| Constant current method                  | It has ability of limited current to prevent the over current of initial charge | It is easy to overcharge in later stage     |
| Constant voltage method                  | It has ability of limited voltage to prevent the over voltage                   | It is easy to over current in initial stage |
| Constant current/constant voltage method | It can limit voltage and current  | Charge time is too long                     |
| Pulse charge method                      | It can reduce the polarization to prevent the battery temperature rise          | Control is complex                          |
| Reflex charge method                     | It can reduce the polarization to prevent the battery temperature rise          | Control is complex                          |

## 2.4 Time Delay Control

A controller is a device, possibly in the form of a chip, analogue electronics, or computer, which monitors and physically alters the operating conditions of a given dynamical system. Many controllers have been developed, that can be divided into two classifications, passive and adaptive power controller. The example for passive power controller is hysteresis, relay and sliding mode control and for adaptive power controller is PID, fuzzy, P-resonant, Time delay controller. Each of them has their advantages, such as simple structure and low maintenance cost.

Adaptive controller is a controller that can modify its behavior in response to changes in the dynamics of the process and the disturbances. A great number of industrial control loops are under adaptive control. These include a wide range of applications in aerospace, process control, ship steering, robotics and other industrial control systems [16]

The time delay is generally regarded as a irritation to a control system. Its presence hinders the control system design, limits the achievable performance of a controller, and may trigger serious stability concerns. As the inverse of time delay implies prediction into the future, the resulting controller exhibits predictive characteristics. Essentially, the time delay controller proposed includes a delay element in positive feedback and a reference model in the forward path. In order to solve the problem of adaptive tuning of the time-delay controller, the dynamics of the system are first identified by the polynomial identification [16].

The proposed controller uses the delay element in positive feedback with a reference model  $G_m(s)$ , as shown in Figure 2.13.

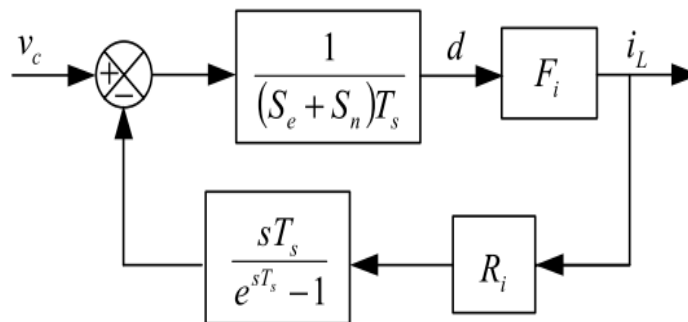


Figure 2.13: Ridley's model of the time-delay controller.

The effects of the sampling and computational time delay, which is an inevitable characteristic of digital control systems, and dead-time, which must be inserted to prevent a leg short circuit, influence the ability of a current controller to effectively track the reference current signals. This is especially evident in a shunt active power filter application where the performance is directly dependent on the ability of the converter to effectively track the reference current signals.

The time it takes to sample the current and voltage values and the time that the DSP takes to process the sampled values leads to a 1 sampling period ( $T_s$ ) time delay between sampling and actually applying the duty cycles to the inverter. This can cause oscillations in the actual current [17].

Lead-acid battery use Traditional Charging Method, they are Constant current, Constant Voltage, constant current constant voltage (CC, CV) and pulse charging constant [18]. Constant currents are used to charge the battery. This method is simple that using current monitoring, however monitoring the voltage of battery is to prevent the over-discharging by higher voltage.

Constant voltage is used to charge the battery. This method is easy to implement but only the initial current required limiting to protect the charger. The drawback of this method is the charging time longer than Constant Current method.

Combine the two methods, CCCV charging method is established. Constant Current is used at initial stage for providing starting charging current. Until the voltage charge up to cutoff or preset voltage, battery is switched to Constant Voltage mode to be a float charge.

Similar to Constant Current method but the pulsed current is used to inject to battery. It is given a relax time in each charging cycle. Using this method can neutralize the internal electrolyte of battery and enhance the life cycle of it. Also the large pulse current can decrease the charging time of battery.

## 2.5 Arduino

A central controller (our Arduino board) receives user commands to execute. It has Internet connectivity through an Ethernet shield mounted on the Arduino. On the user side, a mobile device provides interface with the system as a whole through a user-friendly application. The mobile device can be either wired to the central controller (through USB cable for instance), or communicates with it wirelessly. Within the scope of the home, wireless connectivity can be achieved using an Ethernet shield on the central controller. This way, we would be able to access the controller either locally or remotely through the Internet.

In recent years Arduino – like platforms have seen enormous diffusion both in amateur applications and in research environments due to their simplified programming language and low-cost. The spreading of the new open hardware platform led to an increase of available “interface shields”; this increased furthermore the flexibility of the Arduino platforms which started to spread in most of the academic environments. In the development of control loops for power electronic converters, the platform was not really successful probably due to the limited performances of the microcontrollers which the boards are based on or the lack of availability of suitable interface boards for power electronics.

For increasing the performance of the Arduino – like platforms the replacement of the original microcontroller on ChipKit Uno32boards with a more performance dsPIC which performance are similar to the TI platform. The interface board can be operated with the desired core and simply programmed with the available tools from the manufactures (e.g. Texas Instruments Code Composer Studio or Microchip MPLAB). The developed interface board was used for generating test signals and characterizing the switching performance of 1200 V Si and SiC power semiconductors [19].



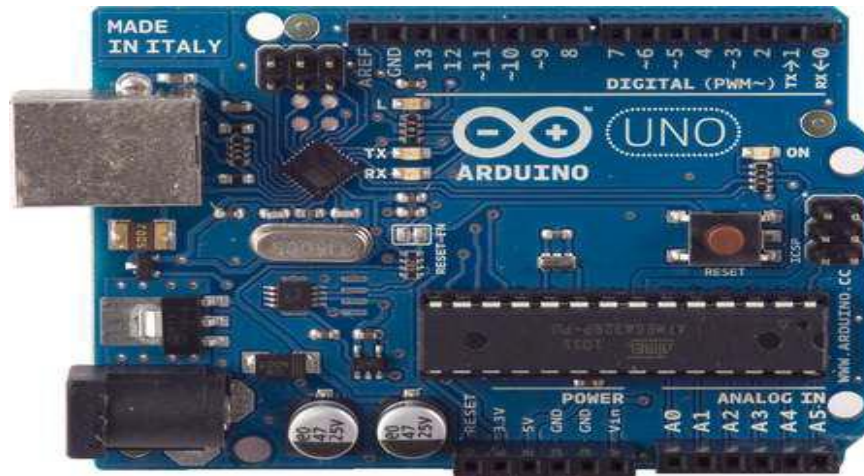


Figure 2.14: The Arduino board

## CHAPTER 3

### RESEARCH METHODOLOGY

#### 3.1 Block Diagram of the Project

Figure 3.1 shows a simplified block diagram of a typical lead-acid batteries charger system. It consist of 5 mains parts as a DC power source, a buck-boost converter, a custom data acquisition system (current sensor) and a control system (consist of Arduino, Matlab and gate drive) and output (battery 12 – 7 Ah).

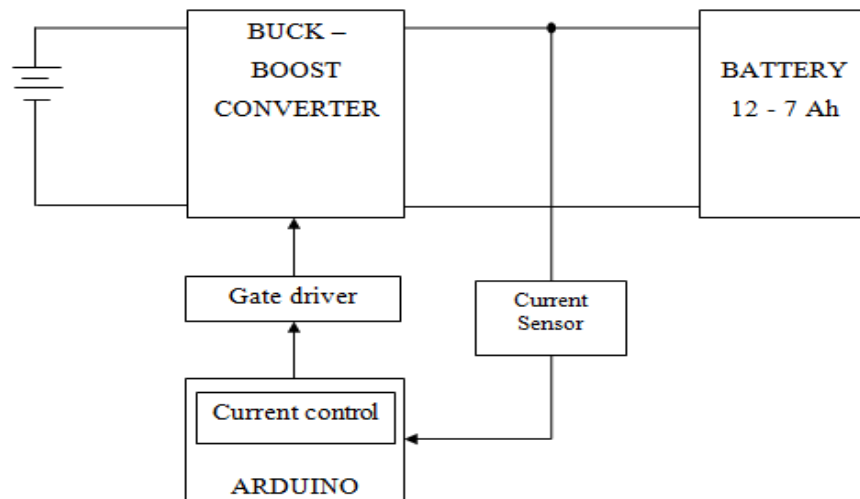


Figure 3.1: Block diagram of time delay control current for battery.

When the input dc voltage is applied to the whole system of the block diagram, a buck – boost converter circuit will convert from unstable DC voltage to stable DC voltage for battery. The two switch converter will be used because PWM will be fed from the controller.

A time delay controller is used by using the current source control technique. The controller will compare the battery current with the reference current. If there have an error, the controller will generate the pulse width modulation (PWM) to feed into a buck – boost converter and rescale the output of battery. This process will continuous until the error approximately to zero to charge the battery efficiently.

## 3.2 Flowchart of System

### 3.2.1 Lead Acid Battery Charger

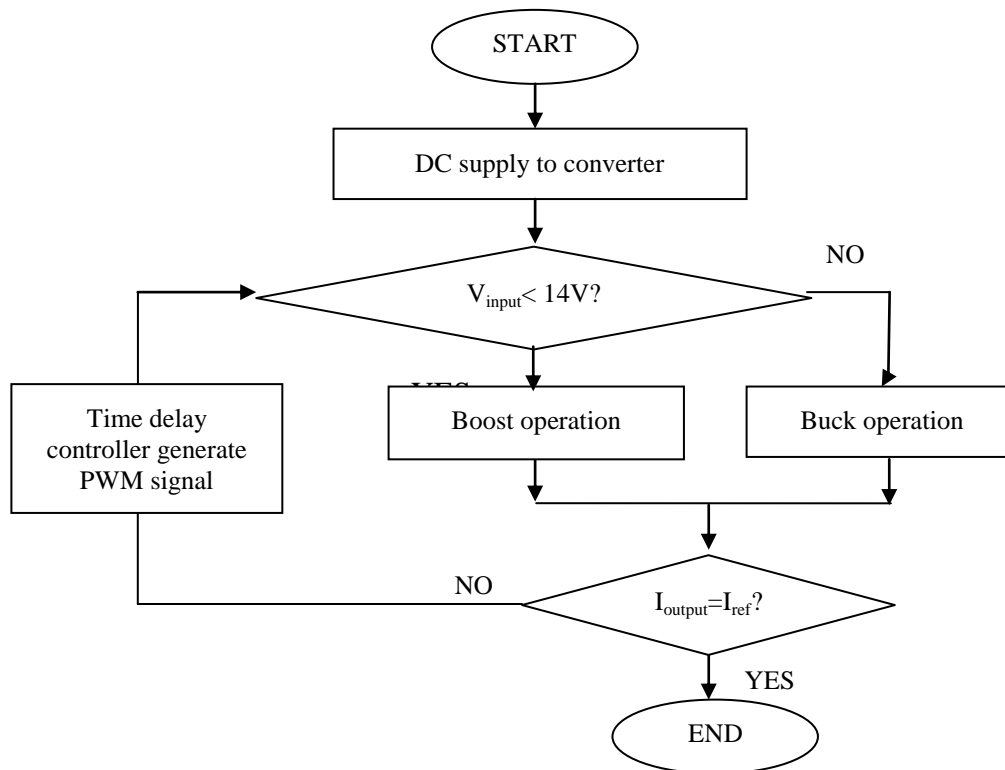


Figure 3.2: Flowchart of the lead acid battery charger

## REFERENCES

- [1] W. Luo, Y. Yang, H. Li, and Y. Jiang, "Design of intelligent battery charger based on SCM double closed-loop control," *2013 IEEE Int. Conf. Mechatronics Autom.*, pp. 1413–1418, Aug. 2013.
- [2] M. Milanovic, A. Roskaric, and M. Auda, "Battery charger based on double-buck and boost converter," in *ISIE '99. Proceedings of the IEEE International Symposium on Industrial Electronics (Cat. No.99TH8465)*, 2000, vol. 2, pp. 747–752.
- [3] C. Mi, "Fast battery equalization with isolated bidirectional DC-DC converter for PHEV applications," *2009 IEEE Veh. Power Propuls. Conf.*, pp. 78–81, Sep. 2009.
- [4] D. Kim, S. Choi, S. Kim, and B. Choi, "MATLAB-based digital design of current mode control for multi-module bidirectional battery charging/discharging converters," *8th Int. Conf. Power Electron. - ECCE Asia*, pp. 2256–2260, May 2011.
- [5] L. Chen, J. Chen, N. Chu, and G. Han, "Current-Pumped Battery Charger," *IEEE Trans. Ind. Electron.*, vol. 55, no. 6, pp. 2482–2488, Jun. 2008.
- [6] C. Alaoui and Z. M. Salameh, "Experiments in fast charging lead acid electric vehicle batteries," *2003 IEEE 58th Veh. Technol. Conf. VTC 2003-Fall (IEEE Cat. No.03CH37484)*, pp. 3326–3331 Vol.5, 2003.
- [7] A. C. Hua and B. Z. Syue, "Charge and discharge characteristics of lead-acid battery and LiFePO<sub>4</sub> battery," in *The 2010 International Power Electronics Conference - ECCE ASIA -*, 2010, no. 95, pp. 1478–1483.
- [8] R. Saiju and S. Heier, "Performance analysis of lead acid battery model for hybrid power system," *2008 IEEE/PES Transm. Distrib. Conf. Expo.*, pp. 1–6, Apr. 2008.
- [9] J. Marcos, J. Dios, A. M. Cao, J. Doval, C. M. Penalver, A. Nogueiras, A. Lago, and F. Poza, "Fast Lead-Acid Battery Charge Strategy," in *Twenty-First Annual IEEE Applied Power Electronics Conference and Exposition, 2006. APEC '06.*, 2006, pp. 610–613.

- [10] J. Alvarez, J. Marcos, A. Lago, A. A. Nogueiras, J. Doval, and C. M. Penalver, "A fully digital smart and fast lead-acid battery charge system," in *IEEE 34th Annual Conference on Power Electronics Specialist, 2003. PESC '03.*, vol. 2, no. 1, pp. 913–917.
- [11] H. Ito, "Disturbance and Delay Robustness Guarantees of Gradient Systems Based on Static Noncooperative Games With an Application to Feedback Control for PEV Charging Load Allocation," *IEEE Trans. Control Syst. Technol.*, vol. 21, no. 4, pp. 1374–1385, Jul. 2013.
- [12] A. Mirzaei, A. Jusoh, Z. Salam, E. Adib, and H. Farzanehfard, "A Novel Soft Switching Bidirectional Coupled Inductor Buck-Boost Converter for Battery," pp. 195–199, 2011.
- [13] T. Feng, Q. Li, F. Wang, and W. Zhang, "Verification and implementation of the non-inverting buck-boost converter in energy-harvesting battery charger," in *2012 7th IEEE Conference on Industrial Electronics and Applications (ICIEA)*, 2012, pp. 855–859.
- [14] K. Goto, Y. Imamura, and M. Shoyama, "Dynamic characteristics model of bi-directional DC-DC converter using state-space averaging method," in *Intelec 2012*, 2012, pp. 1–5.
- [15] Z. Xu, W. Xu, Y. Yu, and Q. Wu, "A study on the stability of current-mode control using time-delay model of pulse-width-modulator," *2008 Asia Simul. Conf. - 7th Int. Conf. Syst. Simul. Sci. Comput.*, vol. 2, no. 2, pp. 1432–1435, Oct. 2008.
- [16] K. M. Tsang, W. L. Lo, and a. B. Rad, "Adaptive time-delay controller," *IEEE Trans. Ind. Electron.*, vol. 47, no. 6, pp. 1350–1353, 2000.
- [17] M. G. F. Gous and H. J. Beukes, "Time delay and dead-time compensation for a current controlled four-leg voltage source inverter utilized as a shunt active filter," *Conf. Rec. 2004 IEEE Ind. Appl. Conf. 2004. 39th IAS Annu. Meet.*, vol. 1, pp. 115–122, 2004.
- [18] T. K. Cheung, K. W. E. Cheng, H. L. Chan, Y. L. Ho, H. S. Chung, and K. P. Tai, "Maintenance techniques for rechargeable battery using pulse charging," *2006 2nd Int. Conf. Power Electron. Syst. Appl.*, pp. 205–208, Nov. 2006.
- [19] R. Pittini, Z. Zhang, and M. A. E. Andersen, "An interface board for developing control loops in power electronics based on microcontrollers and DSPs Cores - Arduino /ChipKit /dsPIC /DSP /TI Piccolo," in *2013 IEEE 14th Workshop on Control and Modeling for Power Electronics (COMPEL)*, 2013, pp. 1–7.

- [20] Y. Li, M. Tsai, C. Tseng, and Y. Chiang, "Model reference adaptive control design for the buck-boost converter," in *IECON 2012 - 38th Annual Conference on IEEE Industrial Electronics Society*, 2012, pp. 543–548.
- [21] R. Herzer, S. E. GmbH, and C. Kg, "Integrated gate driver circuit solutions," pp. 16–18, 2010.
- [22] J. Bernstein and C. Smidts, "Study of the Impact of Hardware Fault on Software Reliability," *16th IEEE Int. Symp. Softw. Reliab. Eng.*, pp. 63–72, 2005.
- [23] J. Hill and C. Nwankpa, "Hardware platform for testing battery energy storage systems in the presence of renewables," *2013 IEEE Grenoble Conf.*, pp. 1–6, Jun. 2013.